AFOSR-TR-97-0484

REPORT DOCUMENTATION PAGE	Form Approved OMB No. 0704-0188

1. AGENCY USE ONLY *(Leave blank)*	2. REPORT DATE	3. REPORT TYPE AND DATES COVERED
	October 15, 1995	Final Technical Report 01 Jul 92 to 30 Jun 95

4. TITLE AND SUBTITLE
Fundamental Studies on the Mechanical Behavior and Fracture characteristics of Metal-Ceramic Interfaces

5. FUNDING NUMBERS
F49620-92-J-0277

6. AUTHOR(S)
K. M. Mukai
A. K. Ghosh

7. PERFORMING ORGANIZATION NAME(S) AND ADDRESS(ES)
University of Michigan
Ann Arbor, MI 48109

8. PERFORMING ORGANIZATION REPORT NUMBER

9. SPONSORING/MONITORING AGENCY NAME(S) AND ADDRESS(ES)
AFOSR/NA
110 Duncan Ave, Suite B 115
Bolling AFB, DC 20332-8050

10. SPONSORING/MONITORING AGENCY REPORT NUMBER
F49620-92-J-0277

11. SUPPLEMENTARY NOTES

12a. DISTRIBUTION AVAILABILITY STATEMENT
Approved for public release; distribution unlimited.

12b. DISTRIBUTION CODE

13. ABSTRACT *(Maximum 200 words)*

Composite properties are closely related to the strength of the interface between the matrix and reinforcement. There is a need for a fundamental level of understanding of the strength characteristics and the origin of failure of the interface since it is the means by which load is transferred from the matrix to reinforcement.

Extended from our previous phase of this study of the interface between ductile and brittle phases under mode II loading,[4] an offset shear geometry was chosen to investigate the strength and fracture behavior of a copper/alumina sandwich. This particular geometry has advantages since it is simple to fabricate and can provide mixed mode information about strength.

In this phase of the study, an attempt has been made to characterize the shear debond strength of metal-ceramic interfaces by use of the offset shear specimen. Specimens with interface precrack geometries as well as those without precracks were tested to examine crack propagation and initiation effects. The goal is to characterize mechanisms of damage initiation at the interface prior to crack propagation using copper-alumina laminates loaded in compression. During each test, crack initiation information was obtained from critical stress to initiate fracture and propagation information was determined from the energy requirement for subsequent crack propagation.

14. SUBJECT TERMS	15. NUMBER OF PAGES
	41
	16. PRICE CODE

17. SECURITY CLASSIFICATION OF REPORT	18. SECURITY CLASSIFICATION OF THIS PAGE	19. SECURITY CLASSIFICATION OF ABSTRACT	20. LIMITATION OF ABSTRACT
Unclassified	Unclassified	Unclassified	UL

Fundamental Studies on the Mechanical Behavior and Fracture Characteristics of Metal-Ceramic Interfaces

Reported by:

K.M. Mukai and A.K. Ghosh

University of Michigan
Ann Arbor, MI 48109

Research: Conducted under AASERT Program

Grant: No. f49620-92-J-0277

Grant Monitor: Dr. A.H. Rosenstein, AFOSR

October 10,1995

I Introduction:

Composite properties are closely related to the strength of the interface between the matrix and reinforcement. There is a need for a fundamental level of understanding of the strength characteristics and the origin of failure of the interface since it is the means by which load is transferred from the matrix to reinforcement. In the past there have been numerous studies on the strength characteristics of interfaces using various simplified models such as the 4-pt bend test, compact tension, and single edge-notch.[1] [2] [3] These tests tend to focus mainly on a Mode I type of loading. It is fairly well known that composites generally fail in mixed mode loading (Mode I + Mode II) and often along the interface. Thus it is important to acquire information about the other extreme of loading condition, namely Mode II.

Extending from our previous phase of this study of the interface between ductile and brittle phases under Mode II loading,[4] an offset shear geometry was chosen to investigate the strength and fracture behavior of a copper/alumina sandwich. This particular geometry has advantages since it is simple to fabricate and can provide mixed mode information about strength. A schematic diagram of this geometry is shown in Fig. 1. By varying the thickness of the metal layer (t) and the distance between notches (s), the phase angle (Ψ the ratio of the Mode II to Mode I components of stress) of the composite can be changed. These changes in phase angle can result in changes in the strength of the composite since Mode I loading will result in the lowest interfacial strength and Mode II the highest.

In this particular geometry a simple laminate sandwich structure has two notches cut into the sides of the sandwich, thus putting the sandwiched phase in shear. This particular geometry allows many variables to be changed including sandwich thickness and notch separation, adjustments of which allow phase angle effects to be investigated. Both tension

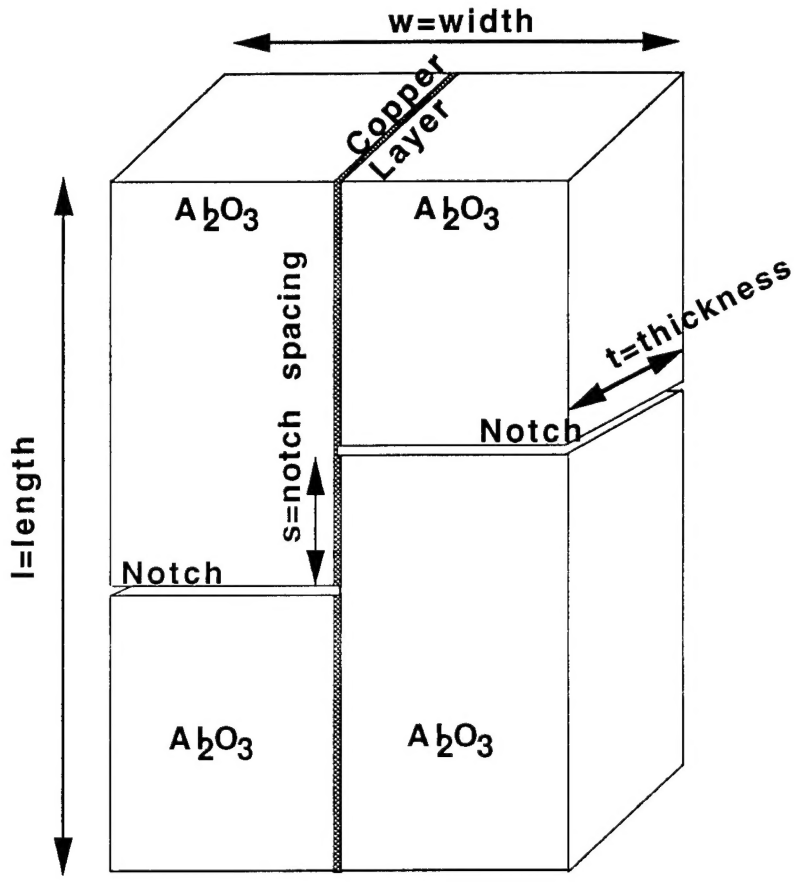

Figure 1. The Offset Shear Geometry with Copper and Alumina. The Copper layer thickness varies as does the notch spacing s. Load axis is vertical.

and compression experiments are possible with this geometry thus subjecting the interface to shear loading with superimposed tension and compression.

In this phase of the study, an attempt has been made to characterize the shear debond strength of metal-ceramic interfaces by use of the offset shear specimen. Specimens with interface precrack geometries as well as those without precracks were tested to examine crack propagation and initiation effects. The goal is to characterize mechanisms of damage initiation at the interface prior to crack propagation using copper-alumina laminates loaded in compression. During each test, crack initiation information was obtained from critical stress to initiate fracture and propagation information was determined from the energy requirement for subsequent crack propagation.

II Materials and Processing

The sandwich laminates used in this study have been fabricated by diffusion bonding of copper and alumina. During bonding, some diffusion of copper atoms occurs into the alumina matrix $\approx 1.6 \times 10^{-8}$ m,[5] but primarily bonding is due to oxygen diffusion into the copper as well as mechanical bonding via flow of the copper into crevices on the alumina surface.[6] The compounds formed at the interface are a $CuAlO_2$ rhombohedral phase and a $CuAl_2O_4$ spinel phase, though there is some controversy over which compound is preferred. [6] [7] [8]

The materials used to fabricate the laminate consisted of an AD-998 alumina plate from Coors Ceramics (Golden, Colorado) and 99.8% pure copper sheets of various thicknesses. The alumina was ground to approximately 4mm thick with a 1500 grit finish then ultrasonically cleaned in acetone and isopropanol to remove most surface contaminants. A second method of preparing alumina plates consisted of polishing to a 6μm finish followed by ultrasonic cleaning. The resulting plates were then placed in an air

furnace and heated to a temperature of 900°C (higher than the bonding temperature used in these experiments) to remove volatiles. They were then cooled and blown off with argon to remove dust or particulate from the surface. Before bonding to a foil of copper, the alumina surface was coated with two molybdenum strips 2500Å thick and approximately 500μm wide were sputtered onto the surface to create a precrack area.

Three thicknesses of copper sheets were used for diffusion bonding: 25μm, 1mm, and 3mm to create shear angles of 89°, 80.5°, and 63.5°, (with respect to specimen transverse direction) respectively.[9] The copper sheets of thickness 1mm and 3mm are ground using SiC to a surface finish of 1000 grit to remove any surface scratches, oxide, and contamination. The 25μm copper sheet was not polished as the other two copper sheets. They were then ultrasonically cleaned in acetone and isopropanol to remove any residual grit or oils from the surface then wiped dry with a Kimwipe and blown off with argon gas to remove any dust from the surface.

The laminate was assembled in air with the copper layer placed in between the two alumina plates. The laminate was then placed in a molybdenum foil bag and lightly sealed by crimping the edges. The bag was then placed in a vacuum furnace and allowed to pump down to a level of 2.0×10^{-5} torr before hot-pressing.

After achieving high vacuum levels, a preload of 1.5 MPa was placed on the composite prior to heating to prevent any contamination that may vaporize from the chamber walls from settling on the bonding surface of the laminate. The chamber was heated to 850°C at a rate of 15°C/minute and held at this temperature for 6-12 hours. When the chamber temperature equilibrated at 850°C, the pressure on the composite was raised to 3MPa for the 1mm and 3mm thick copper composites and 28MPa for the 25μm thick copper composite, and held for the duration of the bonding to achieve a combination mechanical and diffusion bond. At the end of the bonding run, the pressure was kept on the sample and the temperature lowered at a slow rate of 3.5°C/minute to prevent thermal cracking due to a large stress contribution from the CTE (coefficient of thermal expansion)

mismatch of $\Delta\alpha \approx 8x10^{-6}/°C$ between copper and alumina. This mechanism is described in section IV.1. Once the laminate has reached room temperature the load is removed.

The composite was then sectioned on a low speed diamond saw into specimens of approximate dimensions 22x9x7mm for the 1mm and 3mm copper laminates and 11x8x4mm for the 25μm copper laminate. The sides normal to the axial directions were then flattened using a polishing fixture such that they were parallel to one another and normal to the axis.

The notches were cut into the specimen through the alumina and normal to the copper layer on diametrically opposite sides translated by a spacing of approximately 6mm apart for the 1mm and 3mm copper laminates, and 0.75mm and 1.4mm for the 25μm copper laminate with and without a precrack. Initially a low speed diamond saw was utilized until the notch was within a few hundred microns of the copper layer. The notch was then finished by hand using a diamond blade until the notch just touches the copper layer.

III Mechanical Testing

The composite was tested in compression in order to evaluate the shear debond strength and crack propagation characteristics. An Instron 4505 was used in conjunction with an ultra stiff compression loading fixture as shown in Fig. 2. Point loading was used at the top of the fixture in order to ensure a uniform load within the entire fixture.

Teflon sheets 125μm thick covered both the top and bottom platens to minimize frictional effects (μ for teflon ~0.03). The top platen of the fixture was then lowered upon the sample preloading it with 49.5N prior to the start of the test.

A strain gauge extensometer was placed between the platens of the fixture to monitor true sample displacement. Microstrain gauges (approximately 1mm x 0.8mm

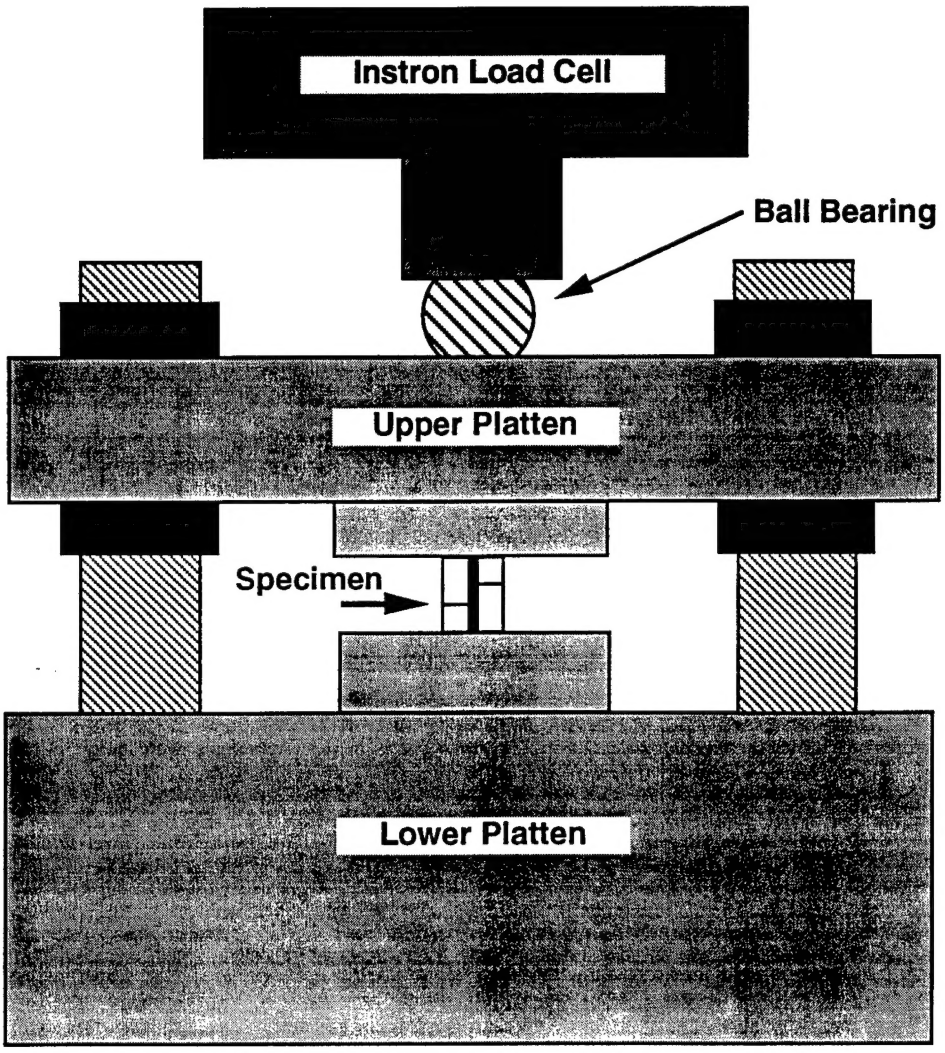

Figure 2. The compression loading fixture.

gauge section), from Micromeasurements (Raleigh, North Carolina) were also placed upon the copper (on the 3mm thick copper laminate) ahead of the notched region oriented normal and parallel, corresponding to the lateral and longitudinal strain gauges respectively, to the loading axis. A preload of 5N is placed upon the fixture to ensure good contact. The fixture was then loaded up to 70N to align the sample in its stiffest possible configuration. It was then unloaded to a preload of 5N in order to begin a test. The sample was loaded at a crosshead speed of 10 μm/minute displaying load curves similiar to Fig. 3a). Typical load curves of these specimens display an elastic load up region followed by a yield point separating the linear and non-linear portions of the curve. This non-linear region leads up to a final peak load followed by either a gradual turnover or a very prominent drop of load. Figures 3a) also displays an ulloading portion of the curve that was used to measure compliance changes.

The 25μm, 1mm, and 3mm copper laminates were loaded both incrementally (as in the case of the 1mm copper laminate) and until either the load turn over point (the load peak) or a load drop was achieved(as in the case of the 25μm and 3mm copper laminates). Upon achieving either criteria, the test was stopped (See figures 3b)-c)) and the laminate was then unloaded instantaneously or in the case of the 1mm copper laminate, the loading was reversed to measure the unloading position of the curve. Micrographs were then taken to characterize deformation and crack length. This type of interrupted testing continued until delamination of the interface was complete. In the case of the 25μm copper laminate, the sample was too small to mount a strain gauge, and the crosshead was the only measurement possible for strain. Fig. 3b) shows the large values for strain due to the sloppiness of the crosshead.

Figure 3a) Typical Loading Curve for Offset Shear Specimens

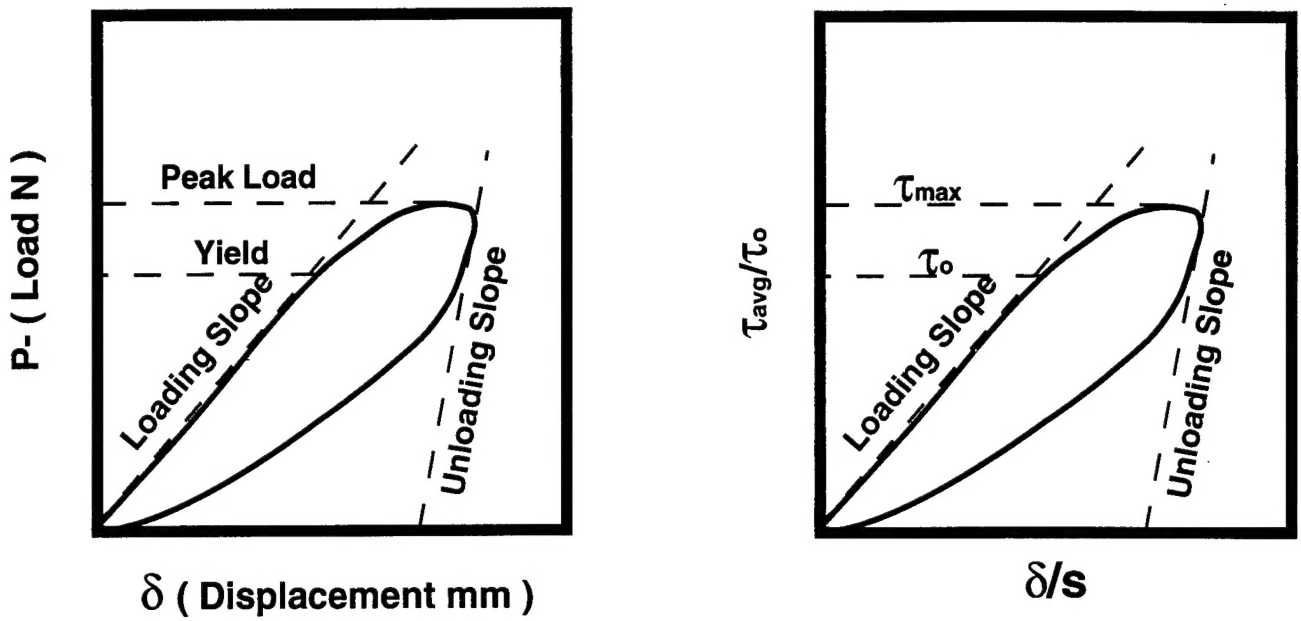

Figure 3a) Example of typical loading curve behavior of an offset shear specimen.

Figure 3b) 25μm Copper Laminate

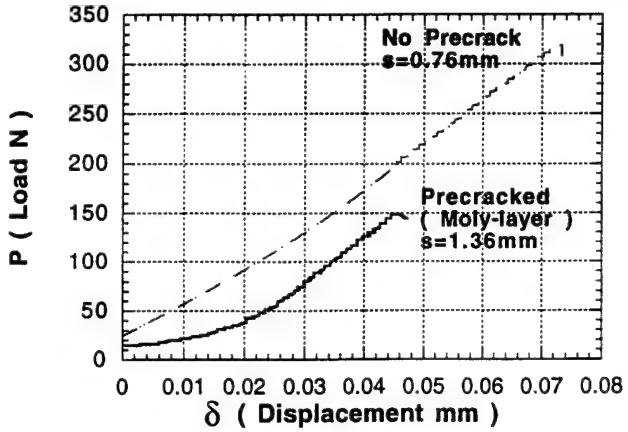

3mm Copper Laminate

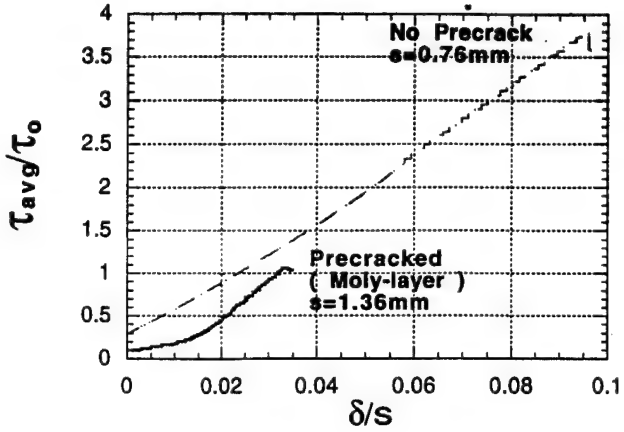

Figure 3c) 1mm Copper Laminate

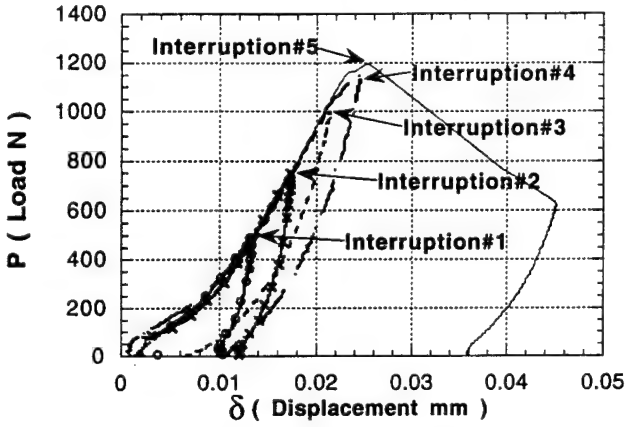

3mm Copper Laminate

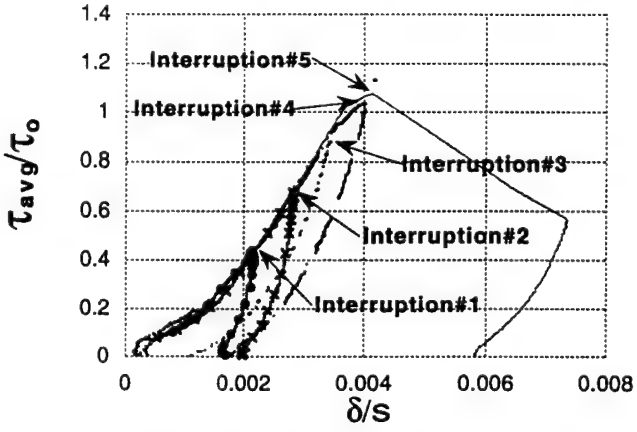

3mm Copper Laminate

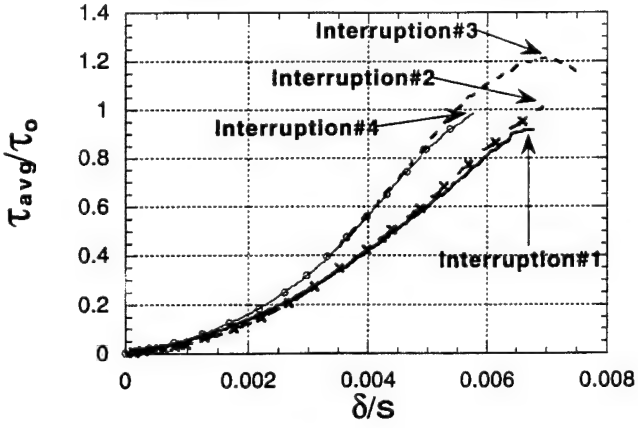

Figure 3c) 1mm Copper Laminate

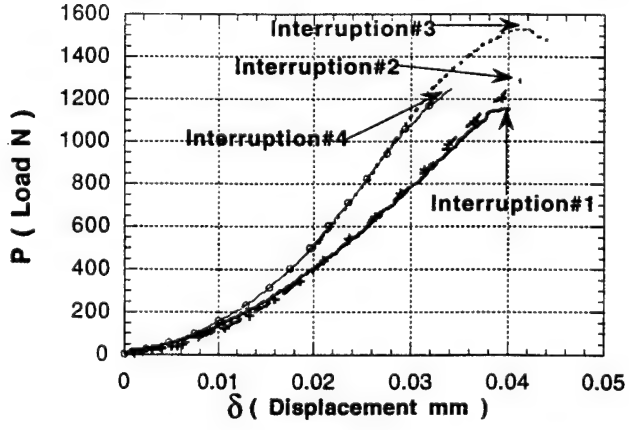

Figure 3 continued) b) 25μm copper laminate (s=0.763mm and s=1.362mm precracked specimen) c) 1mm copper laminate (s=6.14mm) d) 3mm copper laminate (s=5.92mm)

IV Mechanical Properties

IV.1 Residual Stress

For a copper-alumina bond, a large thermal mismatch causes residual stresses to be developed during cooling of the compoiste from the fabrication temperature of 850°C. An estimation of residual stress due to differences in coefficient of thermal expansion, with $\alpha_{Cu}=16.6\text{x}10^{-6}/°C$ and $\alpha_{Al2O3}=8.8\text{x}10^{-6}/°C$, [10]

$$\sigma=E_{Cu}\Delta\alpha\Delta T \qquad (1)$$

the level of stress already at the interface would be σ=765MPa where ΔT=850°C. Since this is above the yield strength of the copper, the maximum possible interfacial residual stress can be on the order of the yield stress of the copper itself, $\sigma_{residual}\approx$60MPa[11]. As the interface itself is already prestressed due to the resiudal tensile stress in the copper, the shear stress for interface fracture may be influenced by this residual stress.

IV.2 Testing Results and Observations:

The laminate specimens were tested in compression until significant changes, such as a yield point, in the loading curve occurred. At such points, the specimen was unloaded and optical microscopy followed. All micrographs taken optically used various degrees of polariziations to enhance surface features. Micrographs were taken at various magnifications to bring out certain surface features for measurements or observation.

Using the load-displacement curves generated for the 25μm, 1mm, and 3mm copper laminates as shown in Fig. 3b)-d), the peak load (P_{peak}) to delamination can be used to find the maximum shear stress τ_{max} at the interface using

$$\tau_{max} = (\frac{P_{peak}}{st}) \qquad (2)$$

where s=spacing between notches and t=thickness of laminate. This results in τ_{max} values for the various laminate thicknesses, as shown in Table I.

Table I.

Maximum Shear and Constraint Ratios

Specimen	Thickness (t)	Ligament Spacing (s)	Maximum Shear Stress (τ_{max})	Constraint Ratio (τ_{max}/τ_o)
3mm Copper Laminate	7.15mm	5.92mm	36.6MPa	1.22
1mm Copper Laminate	6.02mm	6.14mm	32.4MPa	1.08
25μm Copper Laminate	3.69mm	0.76mm	112MPa	3.73
**********	**********	**********	**********	**********
Precracked 25μm copper Laminate	3.43mm	1.36mm	31.9MPa	1.06

τ_{max}=36.6 MPa for the 3mm thick copper layer, τ_{max}=32.4MPa for the 1mm thick copper layer, and τ_{max}=112MPa for the 25μm copper laminate without the precrack and τ_{max}=31.9 with the precrack.

Using Bannister's analysis inwhich he calculated a constraint factor ζ by taking the ratio of the applied stress to the uniaxial yield stress (σ/σ_o) of lead-glass laminates, a similiar analysis can be derived using the ratio of the maximum applied shear stress to the shear yield stress (τ_{max}/τ_o).[9] The results of this analysis are summarized in Table I for a uniaxial yield strength (σ_o) of copper equal to 60MPa (thus the shear yield strength (τ_o) is $\sigma_o/2$). Normalizing τ_{max} with respect to τ_o results in τ_{max}/τ_o=1.22, 1.08, 3.73, and 1.06 for the 3mm, 1mm, 25μm, and precracked 25μm copper laminates respectively.[11] It is important to note that τ_{max} contains any plasticity contributions that have occurred prior to attaining P_{max}.

The compression test of the 3mm copper laminate shown in Fig. 3d) demonstrated how the compliance decreased with multiple interruptions. During interruption#3, at peak stiffness there was a turnover of the load line at τ_{max}=36.6MPa similar to yielding or crack initiation behavior. The results of the microstructure are shown in Fig. 4c). Microscopy revealed cracks at the interface as summarized in Table II.

a) Interruption#1

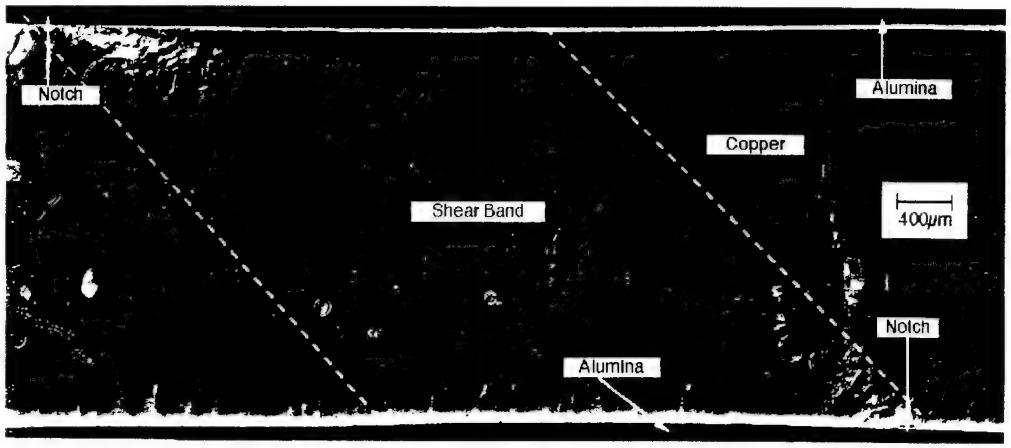

τ_{avg}/τ_o=0.91

δ/s=0.0067

b) Interruption#2

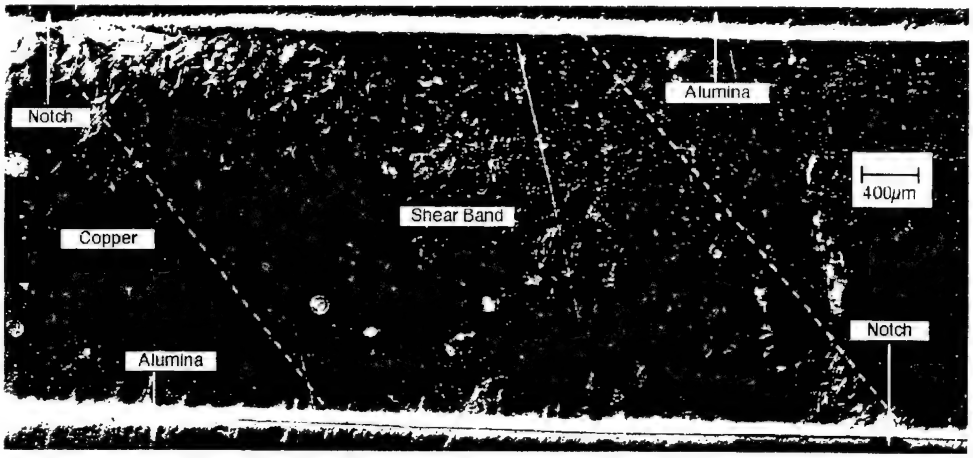

τ_{avg}/τ_o=1.02

δ/s=0.0069

c) Interruption#3

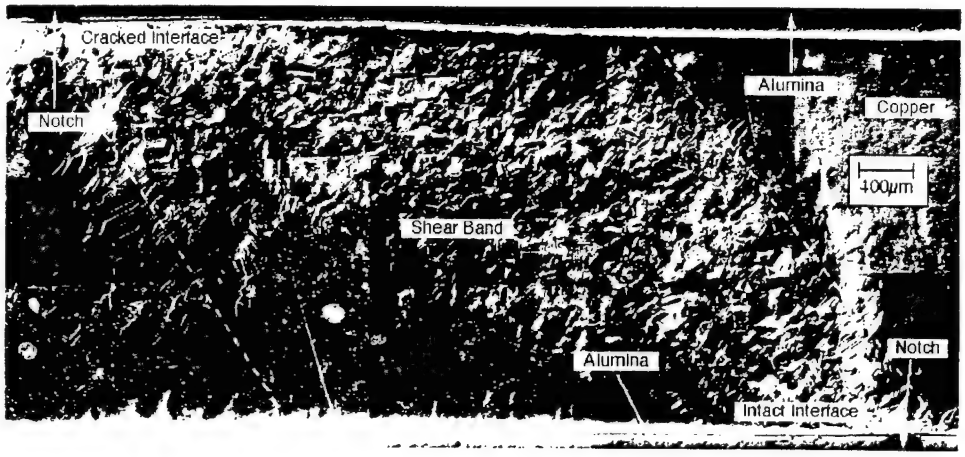

τ_{avg}/τ_o=1.21

δ/s=0.0057

Figure 4) a 3mm copper laminate (s=5.92mm) undergoing compression tests. a) Interruption#1 shear band formation can be seen between the notches, no crack has formed b) Interruption#2 the shear band has become wider and fans out from the notches, no crack has formed c) Interruption#3 the shear band has more texture and the band more width, deformation has become prominent from both notches, and a crack has initiated from the bottom interface

d) Interruption#4

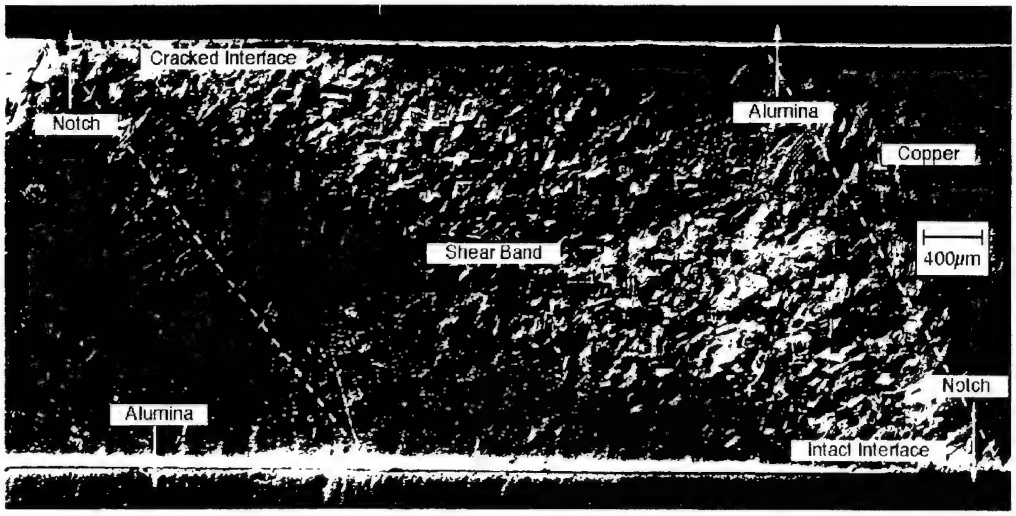

τ_{avg}/τ_o=0.98

δ/s=0.0058

τ_{max}/τ_o=1.40

e) Interruption#5 End of Test δ/s=0.0153

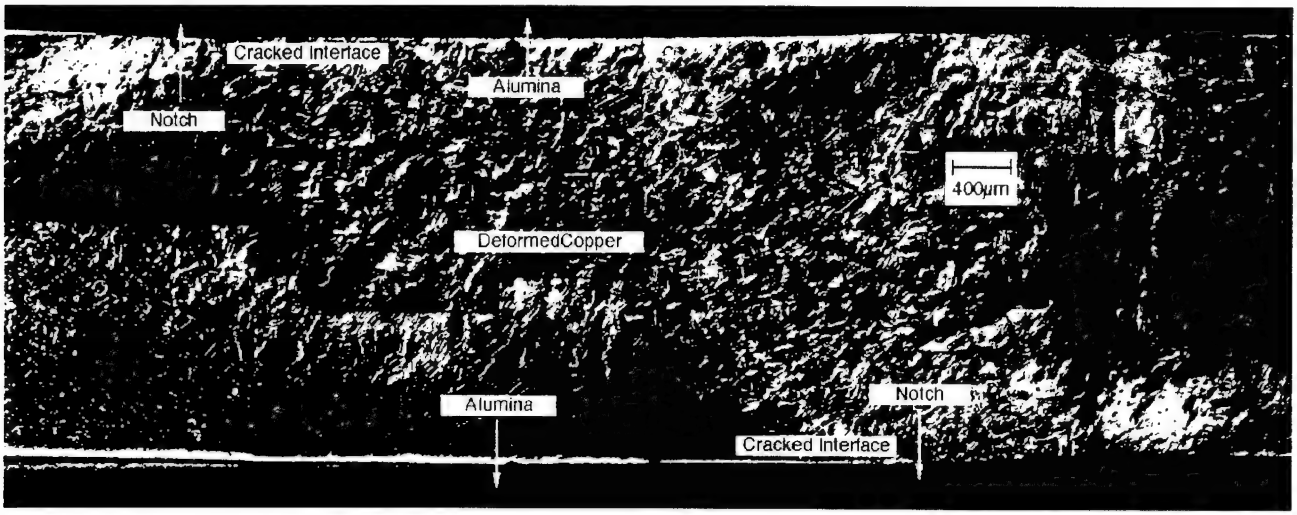

Figure 4 continued d) Interruption#4 deformation has spread beyond the initial shear band into undeformed regions, the crack has propagated along the bottom interface extending approximately the same distance as the deformation has spread e) Interruption#5 final failure of the laminate, both interfaces cracked

Table II.

Crack Lengths

Specimen	Interruption#	Crack Lengths: Notch1 (a_1)	Notch2 (a_2)	Total Crack Length Increase ($\Delta a_1 + \Delta a_2$)
3mm Copper Laminate	2	0	0	
	3	3.02mm	0.41mm	
	4	4.77mm	0.65mm	1.99mm
**********	**********	**********	**********	**********
1mm Copper Laminate	3	38μm	0	
	4	49μm	480μm	491μm
	5	220μm	5.8mm	5.32mm

The cracks were of length a_1=3.02mm and a_2=0.41mm extending from the notches along the interface. Upon reloading of the sample, it was possible to continue the propagation of the cracks. The cracks were grown to lengths of a_1=4.77mm and a_2=0.65mm resulting in an overall change in crack length (Δa) of 1.99mm. No cracks were seen prior to the interruption#3.

The results of compression testing for the 1mm copper laminate can be seen in Fig. 3c) and 5a)-e). As shown in the figure, five interruptions were completed with the fifth interruption resulting in a very large load drop and corresponding strain jump. This

a) Pretesting

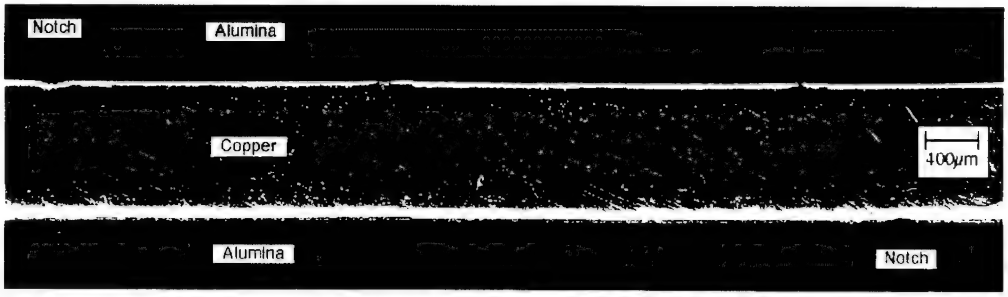

$\tau_{avg}/\tau_o=0$

$\delta/s=0$

b) Interruption #1

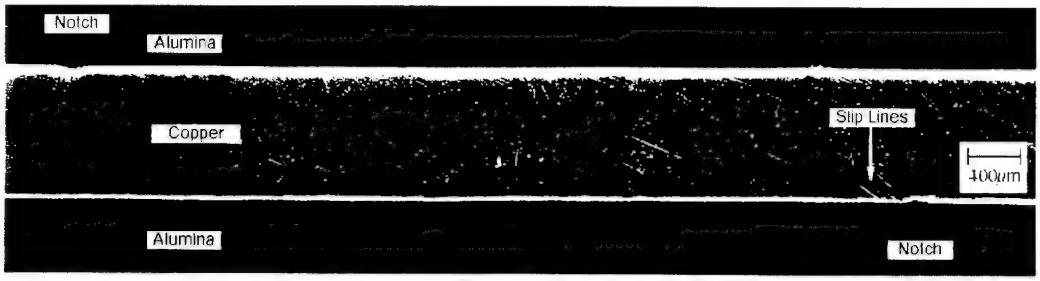

$\tau_{avg}/\tau_o=0.45$

$\delta/s=0.0016$

c) Interruption #2

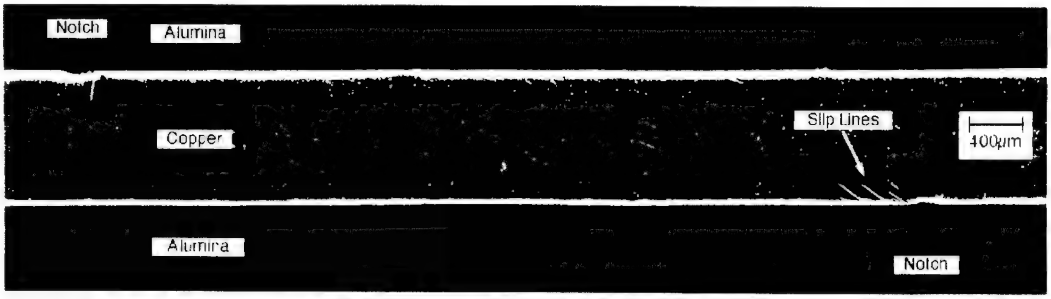

$\tau_{avg}/\tau_o=0.68$

$\delta/s=0.0026$

Figure 5) A 1mm copper laminate (s=6.14mm) undergoing compression tests. a) Pretesting b) Interruption#1 trace slip lines can be seen, no cracking of the interface c) Interruption#2 slip lines have become more prominent, no interface cracking has occured

d) Interruption #3

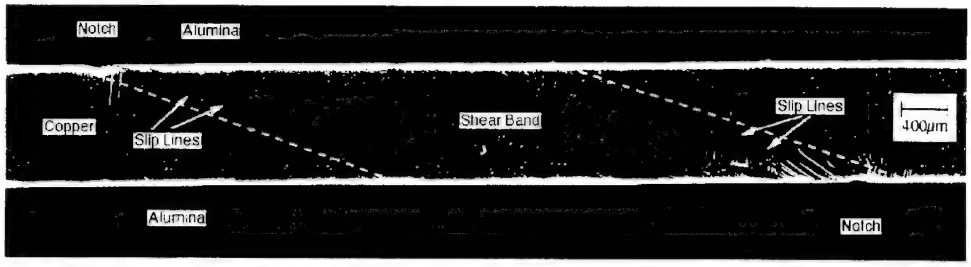

τ_{avg}/τ_o=0.91

δ/s=0.0033

e) Interruption #4

τ_{avg}/τ_o=1.05

δ/s=0.0039

f) Interruption #5

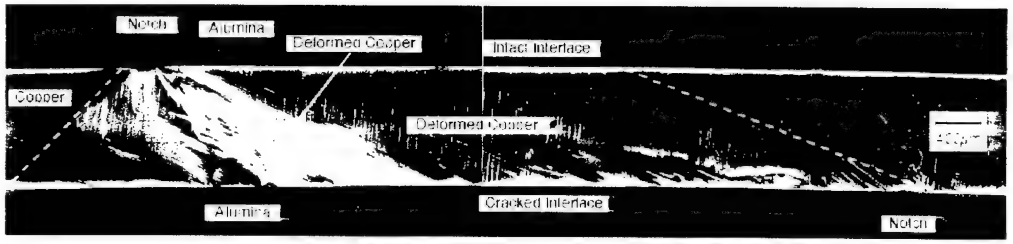

τ_{max}/τ_o=1.08

δ/s=0.0041

Figure 5 continued) d) Interruption#3 shear band formation can be seen, there are no cracks along the interface e) Interruption#4 prominent shear band formation can be seen, the interface has begun to delaminate f) Interruption#5 (end of test) deformation has spread beyond the shear band. the crack has propagated along the upper interface

laminate appeared to have a very small surface crack (a_1=38μm) prior to loading near one of the notches. Upon loading to τ_{avg}/τ_o= 0.68 and 0.91 for interruption#2 and 3, the crack did not move. During interruption#4 at a τ_{avg}/τ_o=1.05 (where τ_{avg} is the P_{peak} for that particular interruption divided by the interfacial area of the ligament, st) the first crack grew to a length of a_1=49μm and a second crack of length a_2=480μm grew from the other notch. The laminate was then loaded for the fifth and final time until the load drop mentioned above and crack extensions of a_1=220μm and a_2=5.8mm resulting in 5.32mm of crack growth Δa. (These results for crack growth are summarized in Table II.).

The 25μm copper laminate appeared to show a peak stress similar to the 1 and 3mm copper laminates. However, it was impossible to see cracks along the interface since the sample was not polished, but cracks can be seen emanating from the notches into the alumina as shown in Fig. 6a). The actual fracture surface, shown in Fig. 6b), shows the alumina still bonded to approximately 50% of the copper surface. Thus cracks formed in the alumina and not on the interface. This is the same result for the precracked 25μm copper laminate shown in Fig 7a). Regardless of where the crack begins, it appears that the cracks will migrate into the brittle alumina phase rather than along the interface when the copper layer is on 25μm thick.

IV.3 Estimates of Interfacial Energy

Using the crack lengths measured above, it is possible to determine the surface free energy of crack propagation $G_{prop.}$ The laminate is loaded to stress levels high enough to propagate cracks and the work under the load displacement curve is calculated using[12]

$$U = \frac{1}{2}\int P d\delta \qquad (3)$$

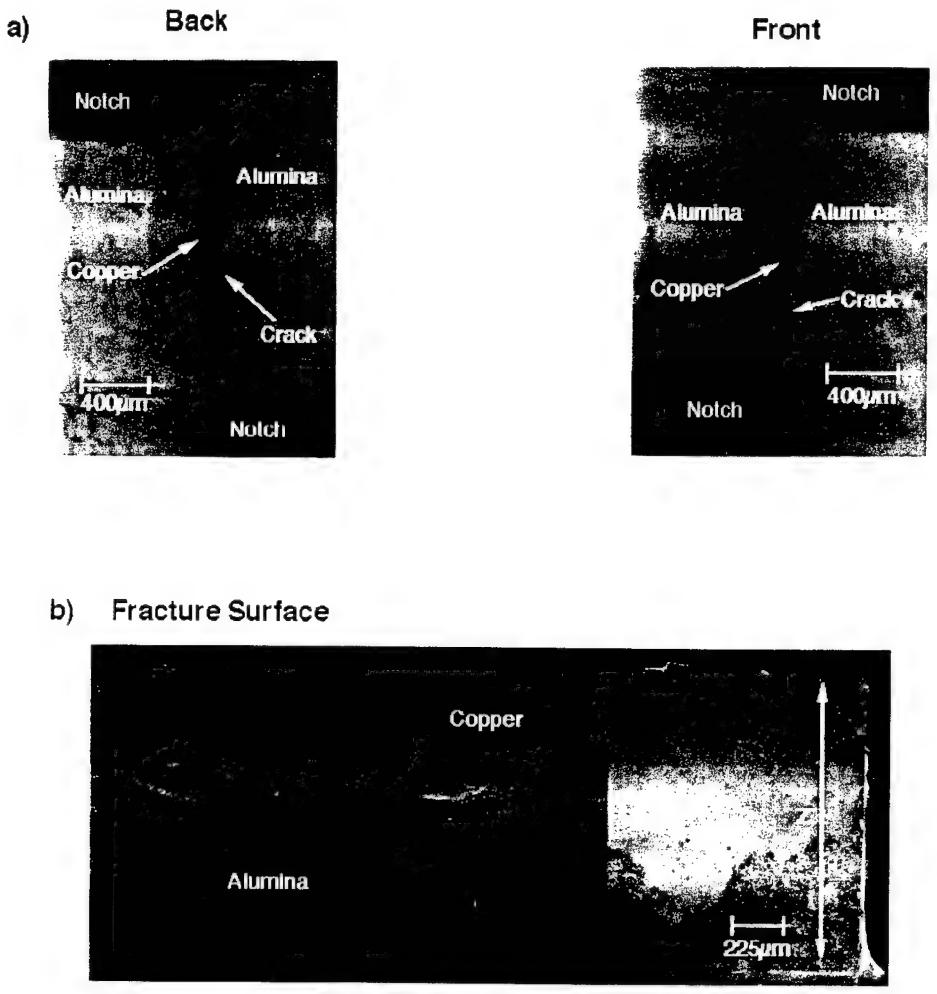

Figure 6 a) a precracked 25μm copper laminate. s=1.4mm showing cracking parallel to the interface but mainly within the alumina b) the fracture surface of the laminate showing the alumina still bonded to the surface. Note: The white haziness in the middle of the picture was caused by shearing of the copper during mounting of the sample.

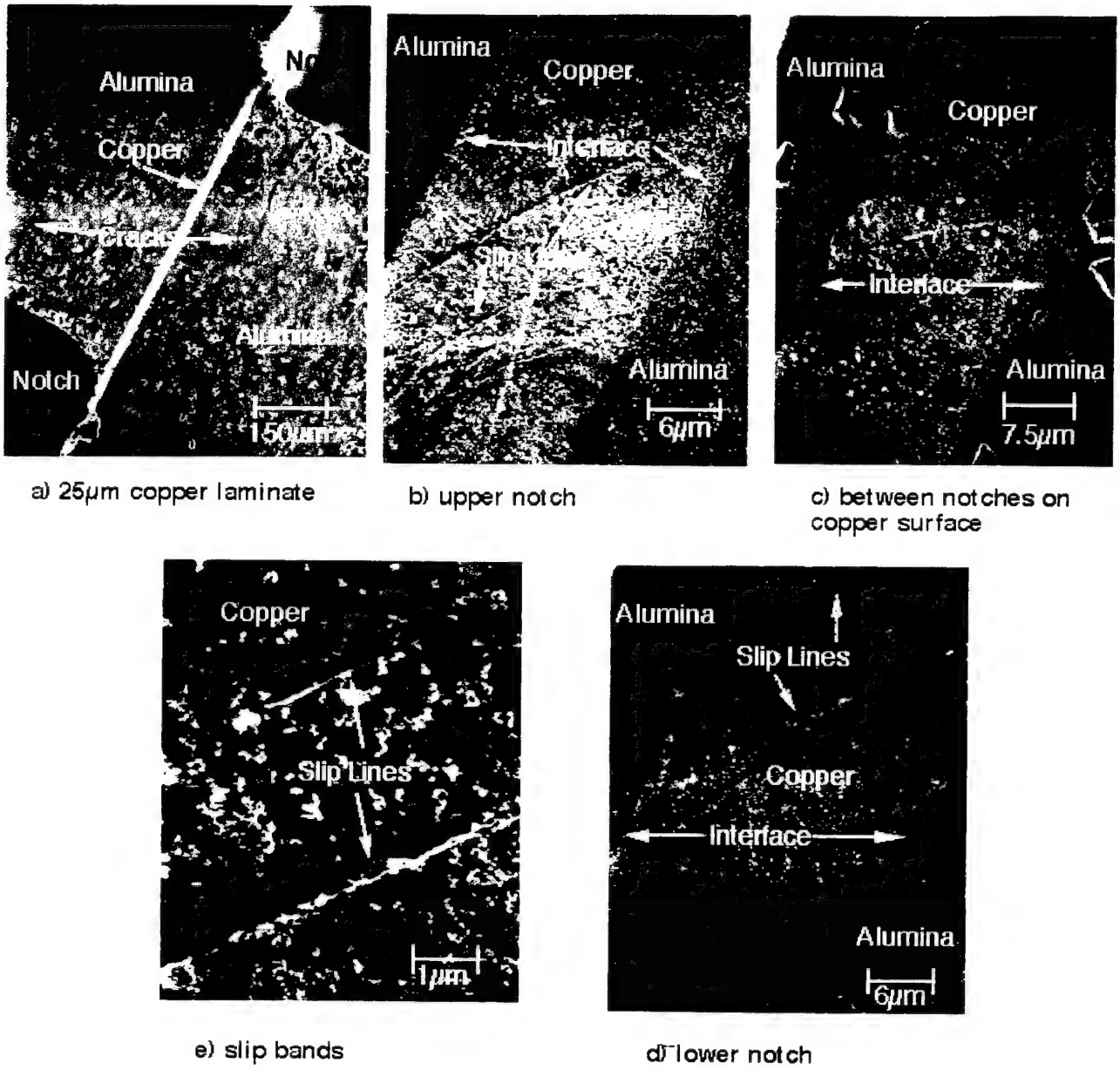

a) 25μm copper laminate

b) upper notch

c) between notches on copper surface

e) slip bands

d) lower notch

Figure 7 a) a 25μm (non-precracked) copper laminate, s=0.76mm, showing cracking in the alumina. The interface was stronger than the alumina b) slip bands formed in the copper near the upper notch c) no slip band formation in the copper located in the middle of the sample between the two notches d) high magnification of the slip bands. Note: cracks can be seen along the interface and in the alumina with little deformation occuring within the copper.

where U=W the work put into the composite, P is the instantaneous load, and δ is the instantaneous displacement, a measure of the fracture propagation energy can be found using[13]

$$G = -\frac{1}{t}\frac{\Delta U}{\Delta a} \qquad (4)$$

where t is the thickness of the composite and a is the crack length. The term G includes all contributions to the load carrying capacity of the laminate including work hardening effects and geometry. Assuming the other effects are negligible, then it can be inferred that all the strain energy goes into delaminating the interface resulting in Eq. (4). In reference to the 3mm copper composite, significant increases in crack length could only be seen after the third and forth interruption. Thus by using the crack lengths measured earlier for interruptions#3 and 4 and the corresponding load-displacement curves, the work of crack propagation can be approximated. This results in a surface free energy of crack propagation of G_{prop}=312 J/m^2 for the 3mm thick copper laminate.

An alternative approach to solving for the same surface energy G_{prop} is to use a linear elastic compliance method. By measuring the load-displacement behavior of the laminate and periodically unloading it and measuring the crack length, it is possible to calculate the G_{prop} for the laminate. This can be achieved by assuming[13]

$$G_{prop} = \frac{P^2}{2t}\frac{\partial C}{\partial a} \qquad (5)$$

where C is the compliance of the specimen upon unloading and P is the maximum peak load (Eq. (5) is valid since it was derived for a plate geometry). The compliance of the load-displacement curves is calculated by taking the inverse of the slope of the unloading line shown in Fig. 3a).[12] Using the data from the 1mm copper laminate, the difference

between the compliance values for interruptions#4 and 5 can be found on Fig. 3c) and the corresponding difference in crack lengths from Table II. Upon substitution into Eq. (5) the surface free energy of propagation was found to be $G_{prop}=85J/m^2$ for the 1mm thick copper laminate (neither the 25μm or 3mm copper laminate data could be used with Eq. (5) since the unloading curves were not measured as shown in Fig. 3b) and 3d)).

IV.4 Microstrain Measurements

The microstrain gauges mounted on the 3mm thick copper laminate have revealed strain build-up in the copper near the interface during testing. Fig. 4a)- e) shows these strains to be in the plastic regime. Fig. 8 shows the level of strain build-up normal and parallel to the loading direction, lateral and longitudinal gauge respectively, just ahead of the notched region. A closer examination of the longitudinal strain reveals the stress lost when the crack propagated is σ=53.7MPa which can be found from [12]

$$\sigma \approx \left(E_{Cu}\varepsilon\right) \qquad (6)$$

where ε represents either longitudinal or lateral strain (ε =0.000537 measured from the logitudinal strain gauge) and E_{Cu} the youngs modulus of copper (E_{Cu}=100Gpa). Normalizing with respect to the uniaxial yield strength of copper resulted in σ/σ_0=0.895. This indicated that the level of total stress within the copper layer was probably above that necessary to cause yielding since ε relief would reduce $\sigma < \sigma_0$.

Figure 8) 3mm Copper Laminate

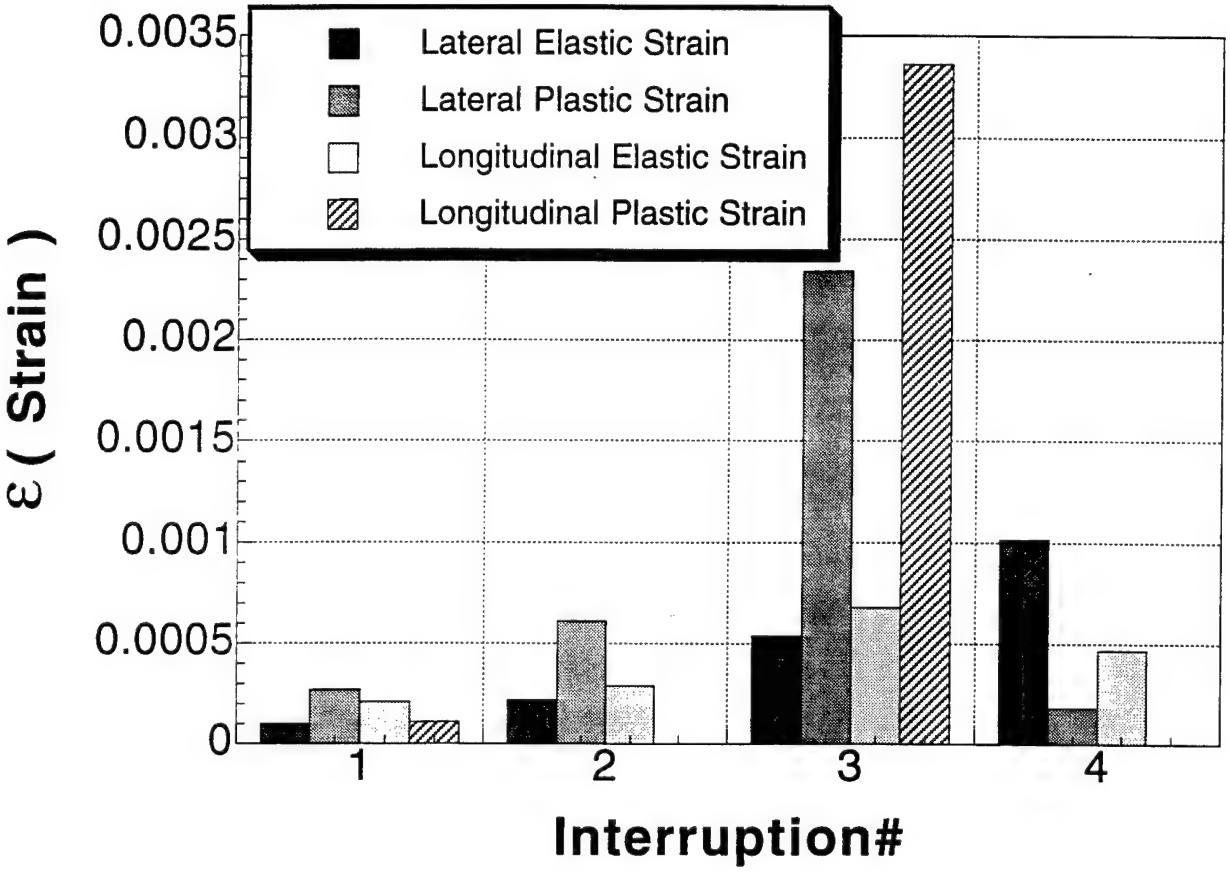

Figure 8) A 3mm copper laminate (s=5.74mm) strain gauge measurement showing large changes in deformation after crack initiation, interruption#3. Strain gauge measurements after interruption#3 are useless since the copper ligament was unconstrained.

IV.5 Slip Band Formation

From the micrographs in Fig. 4, a significant amount of plasticity was observed between the two notches. There is indication of strain localization in an inclined band between the two notches which bears similarity with fracture characteristics along such a path by Bannister et al. in their constrained flow experiments.[9] As the laminate was tested multiple times at higher stresses, the increase in the deformation along the band became more prominent but the band itself did not appear to grow along the interface. It was not until the fourth and final load interruption that the deformation began to spread out beyond this band and into the interface region. This spreading of deformation along the interface appears to coincide with the increase in crack length. It appears that the band expanded about as much as the crack length increased.

The deformation within the 1mm copper laminate also appeared to form a shear band but in a different manner. During the initial loading of the laminate, slip bands could be seen nucleating well below the shear yield stress (τ_o) as shown in Fig. 5b) and c). These bands did not appear to touch the interface but formed in the bulk of the copper and extend to the interfaces. As testing continued, more of these slip lines formed and continued to extend towards the interface with few contacting the interface as shown in Fig. 9. Small slip lines began to form normal to the interface terminating on adjacent grain boundaries thereby enhancing grain boundary visibility. There was no well formed shear band within the copper in this case even after deformation traversed the entire copper layer between the notches. It did appear that some of the very prominent slip lines hitting the interface had caused partial delamination as shown in Fig. 10, but as shown in Fig. 11, the slip had not touched the surface nor had the crack propagated. By interruption#4, the cracks had begun to propagate along the interface delaminating both regions damaged and

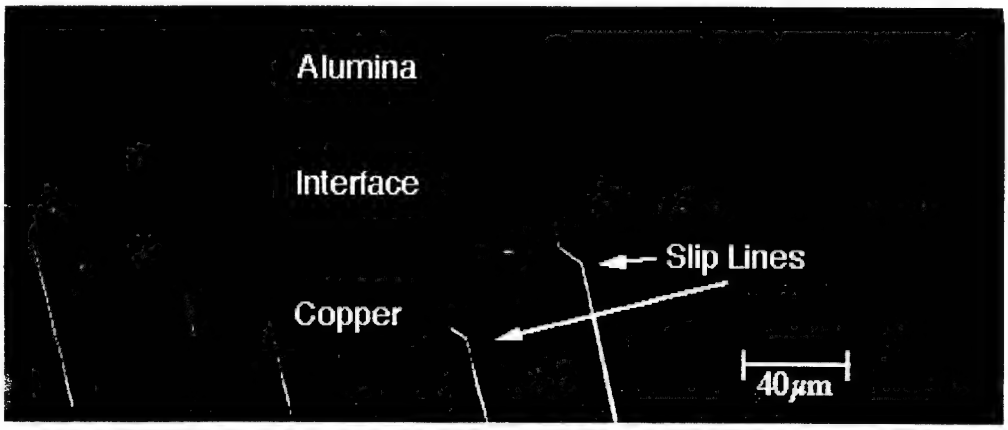

Figure 9) a 1mm copper laminate (s=6.04mm) showing slip lines in the copper approaching the interface but not touching it τ_{avg}/τ_o=0.91.

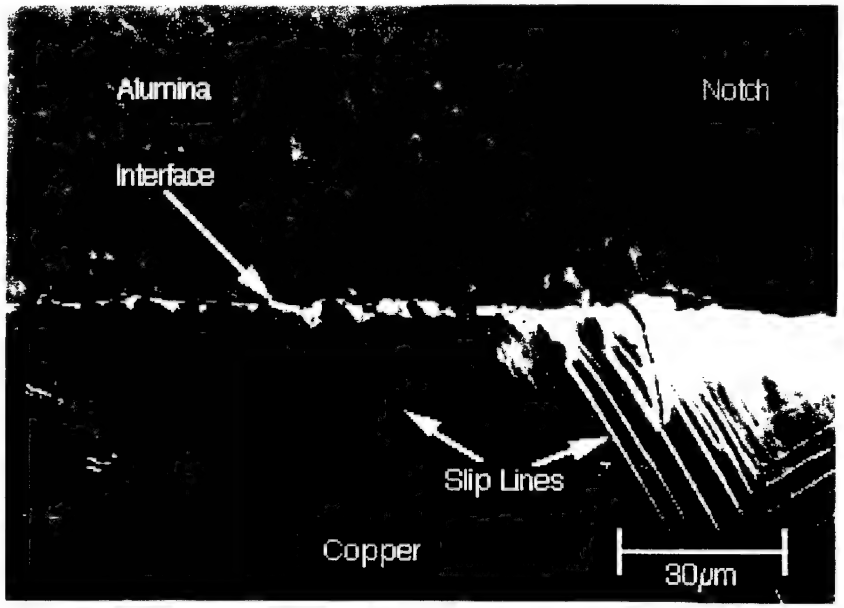

a)

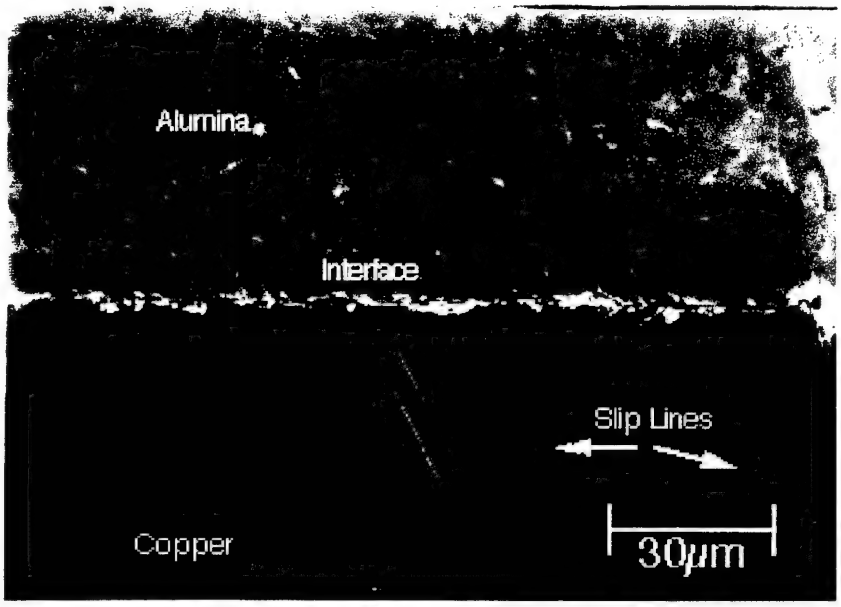

b)

Figure 10) a 1mm copper laminate (s=6.04mm) displaying slip lines apparently touching the interface when loaded to τ_{avg}/τ_o=1.05. a) near a notch b) approximately one centimeter in from the notch

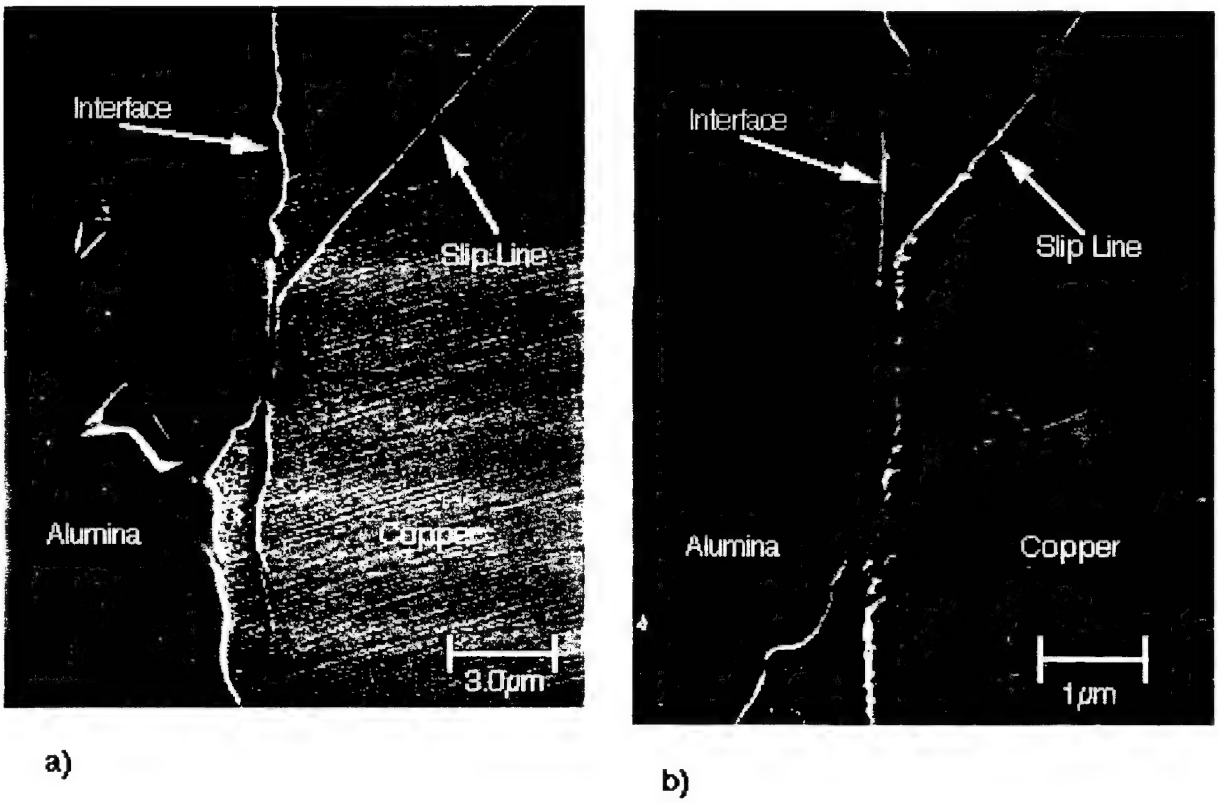

Figure 11) The interface of a 1mm copper laminate (s=6.04mm) displaying a slip line in the copper changing direction due to the constraint caused by bonding with the alumina a) low magnification b) high magnification shows the copper is still bonded to the alumina

undamaged by slip. During interruption#5, the interface delaminated totally thereby relieving the constraint on it. The unconstrained copper readily deformed exhibiting a profusion of slip lines not observed when the copper was constrained.

Fig. 7b)-e) shows the deformation occuring within a 25μm copper laminate. It can be seen that there is no coarse scale slip occuring within the copper phase, but slip lines can be seen just ahead of the notches in Fig. 7b), d), and e). There is no slip observed in the center region between the notches as shown in Fig. 7c). Cracking occurs within the alumina along the interface, but the failures occur by cracking within the alumina parallel to the interface 100-200μm away from the interface as shown in Fig. 7a). The cracks parallel to the interface formed concurrently with those along the interface shown in the Figs. 7b)-d).

V. Discussion

V.1 Constraint Effects

The offset shear experiments have led to several interesting observations. By comparison of the resulting maximum shear stresses for the 1mm and 3mm copper laminates, it would appear that the maximum shear stress increases as the layer thickness decreases since constraint is higher and the shear angle is steeper. However upon comparing 25μm and 1mm copper laminate τ_{max} values it appears that the maximum stres increases with decreasing layer thickness. Thus shear stress distribution is similiar to Bannister's work on lead-glass laminates.[9] The shear stress initially drops with increasing angle of constraint and reaches a minimum, then increases again as found in this work as shown in Table III.

Table III.

Ligament Thickness and Angle of Constraint

Specimen	Ligament : thickness ratio s/t	Angle of Constraint θ°	Maximum Shear Stress τ_{max}
3mm Copper Laminate	2.16	65.16°	36.6MPa
1mm Copper Laminate	6.42	81.15°	32.4MPa
25μm Copper Laminate	30.52	88.12°	112MPa
**********	**********	**********	**********
Precracked 25μm Copper Laminate	54.48	88.95°	31.9MPa

As shown in Table III. the angle of constraint has a parabolic distribution with τ_{max} (in the case of the precracked 25μm copper laminate, though the angle of constraint is high, the maximum shear stress is low compared to the uncracked 25μm copper laminate demonstrating the magnitude of the contribution crack initiation plays on interface toughness measurements.

The constraint values appear to make sense though the actual value may be low. The 3mm copper laminate appeared to have more deformation in the copper than the 1mm copper laminate, thus there had to be less constraint for the 3mm copper laminate though the constraint values do not show it (Note: the constraint is calculated using τ_{max}, thus hardening effects are incorporated into the measurements for constraint). The 25μm

copper laminates did not appear to show any significant deformation in the copper and fractured in the alumina indicating the constraint had to be high and validating the large constraint values calculated above in Table I. It does appear that to get crack propagation along the interface under the bonding conditions used, the constraint cannot be too high otherwise cracking will occur in the alumina. Thus there must be a minimum thickness, and therefore a maximum constraint, for the copper layer at which cracking no longer occurs along the interface, but in the alumina instead.

V.2 Precraking Effects

It appears that there is a correlation between the intact and precracked 25μm copper laminates. There is almost a 70% decrease in the maximum shear strength of the specimens with the precrack compared to those that did not have the precrack. Since the intact samples are supposed to simulate non-damaged samples, it is expected that the composites with the precrack would require less stress to failure. The precracked interface has a very low fracture toughness, $10 J/m^2$ for the bond strength between molybdenum and alumina,[3] that should delaminate with very little stress. Thus it can be assumed that the decrease in shear strength can be attributed in large part to the lack of initiation required to form the crack at the interface.

V.3 Grains Size Effects

It is important to note that in Bannister's experiments, he used samples of the same thickness of metal layer and varied notch spacing to change angles.[9] In these copper/alumina experiments, variations of layer thickness was the only way to create the angles necessary with the limited size of the furnace used. By changing the thickness of

copper layer, the grain size relative to the thickness can begin to play a role. As shown in Table IV. there is a distribution of grain sizes with copper thickness.

Table IV.

Grain Size and Grains per layer Thickness

Specimen	Grain Size (GS)	Grains per copper layer thickness t/(GS)	Angle of Constraint θ°
3mm Copper Laminate	60μm	46	65.16°
1mm Copper Laminate	112μm	9	81.15°
25μm Copper Laminate	15μm	1	88.12°
**********	**********		**********
Precracked 25μm Copper Laminate	15μm	1	88.95°

Using a linear intercept method results in grain sizes of 60μm, 112μm repectively, and 15μm for the 3mm, 1mm, and 25μm copper laminates respectively.[17] Both the 3mm and 1mm copper laminate thicknesses are much larger than the grain size, thus slip can readily occur well within the copper since grain boundaries can be the nucleating sites for slip and the grains can rotate as in Ashby's model of deformation in polycrystals under non-uniform strain.[18] However, it is important to note that the 3mm copper laminate has a more optimal shear angle at 65.16° since it is closer to the optimal 45° for shear than the 1mm copper laminate at 81°. Taking into account the number of grains across the thickness of

the copper, it can be inferred that the 45 grains across the 3mm copper laminate thickness could confine deformation to the slip band much easier than the 9 grains across the 1mm copper laminate. As shown in Fig. 4a) and b) and Fig. 5d) and e), the deformation in the 3mm copper laminate is more confined to the shear band and does not extend to the interface as extensively as the 1mm copper laminate shear band. Thus it is probably easier for slip to be confined to the shear band in the 3mm copper laminate than in the 1mm copper laminate due to a combination of constraint angle and grain size effects.

In the case of the 25μm copper laminate, the lack of fine polish prevented any high magnification surface change examination. However, as shown in Fig. 7b), d), and e) there is some deformation occuring near the notches. However, there is none occuring in the middle of the specimen as shown in Fig. 7c). The constraint of this particular sample is extremely high and does not allow any significant amount of flow to occur prior to fracture of the alumina. This can be verified by Fig. 7a) and 7c) which show cracks in the alumina with no deformation. It appears that it is easier to break the alumina than either flow the copper or break the interface. As shown in Fig. 6b), even the interface retains most of the alumina when the crack is initiated along the interface by the precrack. The crack appears to diverge into the alumina. Thus deformation can be considered absent in the 25μm copper laminate due to the high constraint.

V.4 Deformation Mechanism Results

Due to constraint differences, the 1mm copper laminate displays a somewhat different mechanism of deformation than seen in the 3mm copper laminate. The deformation is not confined to the shear band and tends to form very prominent slip lines that form in the middle of the copper layer and extend normal to the interface. Initially they appear to form within the shear band, but quickly expand out of it, as shown in Fig. 5d) and e). It is possible that the slip normal to the loading direction is indirectly caused by

shearing of grains in the general direction of the shear band. This would produce slip lines within the grain normal to the shearing direction and also parallel between the slip lines. Of course this is orietation dependent, and without the grain orientation information it is difficult to say what is the exact mechanism. It is possible that the slip bands may actually be twins. [14] [21] Though the stress in FCC materials to cause twinning is higher ($\approx 1.15\sigma_o$ where σ_o is the uniaxial yield stress)[15] than that to cause slip, the high level of constraint may prevent slip and force twinning to occur. As shown in Fig. 5e), the suspected twins are almost 800μm long in the middle of the copper, much larger than the grain size. It is possible that some twin like structure has been able to cross grain boundaries in a similiar fashion to the formation of kink-bands. As we saw earlier in Fig. 5a), the annealing twins themselves were hundreds of microns long, so it is entirely possible that a twin structure has formed. Some orientation analysis must follow to find the answer to this question.

The slip lines hitting the interface of the 1mm copper laminate theoretically should form some type of delamination, void, or step. Without this occuring, it would be impossible for the slip lines to hit the interface since the edge of the copper grain bonded to the alumina would be unable to force a dislocation line to form in the alumina. The dislocation line within the copper would be trapped and alternate slip systems would have to be found to accomodate the strain buildup at the interface.[16] Fig. 11 shows that well formed slip lines do appear to deviate from the interface and follow a path parallel to the interface. The copper between the slip line parallel to the interface and the alumina appears to have contracted below the surface, thus there must be some deformation present allowing this to occur. This could be the factor leading to the decrease in maximum shear stress between the 1mm and 3mm copper composites since the extended slip band formation near the interface present in the 1mm copper laminate is absent in the 3mm copper laminate. Thus, even though the crack initiated and propagated in much the same manner as the 3mm copper laminate, the damage from slip along the interface probably

caused the lower maximum shear stress. In additon, using a simple Hall-Petch relation,[19] [20] the yield stress in the 1mm copper laminate would be lower than that of the 3mm laminate simply due to grainsize effects. This lower yield stress would allow more deformation to occur within the copper which, with the larger grains size and thinner layer of copper, would allow more deformatio to reach the interface between the copper and alumina.

According to the micrographs of the 3mm copper laminate, the majority of deformation occurs after the crack has delaminated thereby unconstraining the interface. As shown in Fig. 4a)-d), the deformation increases with rising load, but the extent of propagation of deformation along the interface moves approximately with the crack length. This implies that at this thickness of copper, the stress required to propagate the crack is less than the coarse sclae yield stress under these constraint conditions. According to Ashby et al., the constrained flow stress is higher under constraint than in uniaxial tension,[16] thus it is certainly possible that there may be minimal coarse scale deformaton occurring ahead of the crack tip since the maximum shear stress is less than the flow stress in uniaxial tension.

Although the copper surfaces show some deformation, it is impossible to see its effects on the load-displacement figures. As shown in Fig. 5b)-f), there is significant deformation on the surface yet no change in slope of the Fig. 3c). Until the cracks are moving, there is no significant change in the compliance of these laminates. To an extent, the plasticity occuring coincidentally with crack propagation may be negligible. The residual plastic strain on the copper surface just ahead of the crack tip has been measured to be at most 0.07% on the surface just prior to crack propagation (Interruption#2) along the interface as shown in Fig 8 At this very minute level of plastic strain it is certainly within reason to suspect that the plasticity can be neglected in the surface free energy calculations from section IV.3.

V.5 Surface Free Energy Results

With the above reasoning, the surface free energy values measured are within reason considering the mode and means by which failure occured. A surface free energy of G_{prop}=312J/m^2 for the 3mm copper laminate is reasonable. Cannon et al. have published values on the order of G_{prop}=150 J/m^2 by testing in mode I using SEN specimens and bonding conditions.[1] As expected, the surface free energy should increase in mode II compression testing. However, the results of the 1mm thick copper specimen are subject to some skepticism since G_{prop}=85J/m^2 which is significantly lower than both the mode I value and the previous value for mode II surface free energy G_{prop}=312J/m^2 the 3mm copper laminate. Though there are some slight loading differences between the 1mm and 3mm laminate, the value for the surface free energy of propagation should still remain greater than the mode I value. However, the type of bonding does make a difference in the strength of the bond. According to a Beraud et al., temperature makes a very large difference in the strength of diffusion bonds with the ultimate strength coming from liquid state bonds.[6] It may not necessarily be the case that the mode II surface free energy of the 1mm copper laminate has to be higher than the mode I surface free energy from reference 1 since the bonding conditions are not the same.

The lower mode II surface free energy for the 1mm thick copper laminate could be a result of the methodology by which the crack moved. As described in section V.2, the slip bands of the 1mm copper laminate had already begun to damage the copper near the interface ahead of the crack tip thereby weakening the interface. The load drop by which the crack moved in the 1mm copper laminate was very sharp in comparison to the 3mm laminate which failed under much more controlled load dropping. It is certainly possible that the interface may have been significantly weakened by the slip occurring at the interface ahead of the crack tip.

V.6 Microstrain Gauge Results

Looking at the microstrain gauge results in Fig. 8, it can be shown that when the crack in the 3mm thick copper laminate propagated it caused a stress decrease of 53.7MPa of elastic stress due to elastic strain. This implies that the stress required to initiate the crack exceeded the uniaxial yield stress and the crack propagated at stress levels above the yield stress. As seen in Fig. 4c) and d), the deformation moves with the crack-tip. The same behavior can be seen in the 1mm thick copper laminate. As shown in Fig. 5a)-f), although there is some slip occurring prior to the crack passing through the slipped region, extensive slip steps are observed after the crack has propagated. The remaining plastic strain in the copper shown in Figs. 4e) and 5f) are a result of deformation after the crack moved through the strain gauge region and the copper no longer was constrained.

It would be useful to correlate the microstrain gauge results with the yield criteria to estimate how close to yielding the laminate reached. By calculating a type of effective strain value, ε_{eff}, using[12]

$$\varepsilon_{eff} = \left(\frac{2}{3}\left(\varepsilon_I^{\,2} + \varepsilon_{II}^{\,2} + \varepsilon_{III}^{\,2}\right)\right)^{\frac{1}{2}} \qquad (7)$$

where we assume ε_I and ε_{II} are the lateral and longitudinal strains respectively, and ε_{III} is 0, an idea of the overall strain values can be used to compare the amounts of strain built up during each test on the 3mm thick copper laminate. This is an indication of the relative amount of strain necessary within the copper layer for the crack to propagate. As shown from Fig. 12, the amount of strain is greater than 0.4% (ε). For coarse scale slip, the expected level of strain would be 0.2% (ε_o) or higher.[14] Since $\varepsilon_o<\varepsilon$, there appears to be significant flow along the interface ahead of the crack-tip just prior to achieving strain levels great enough to generate stresses to crack the interface.

Figure 12) 3mm Copper Laminate

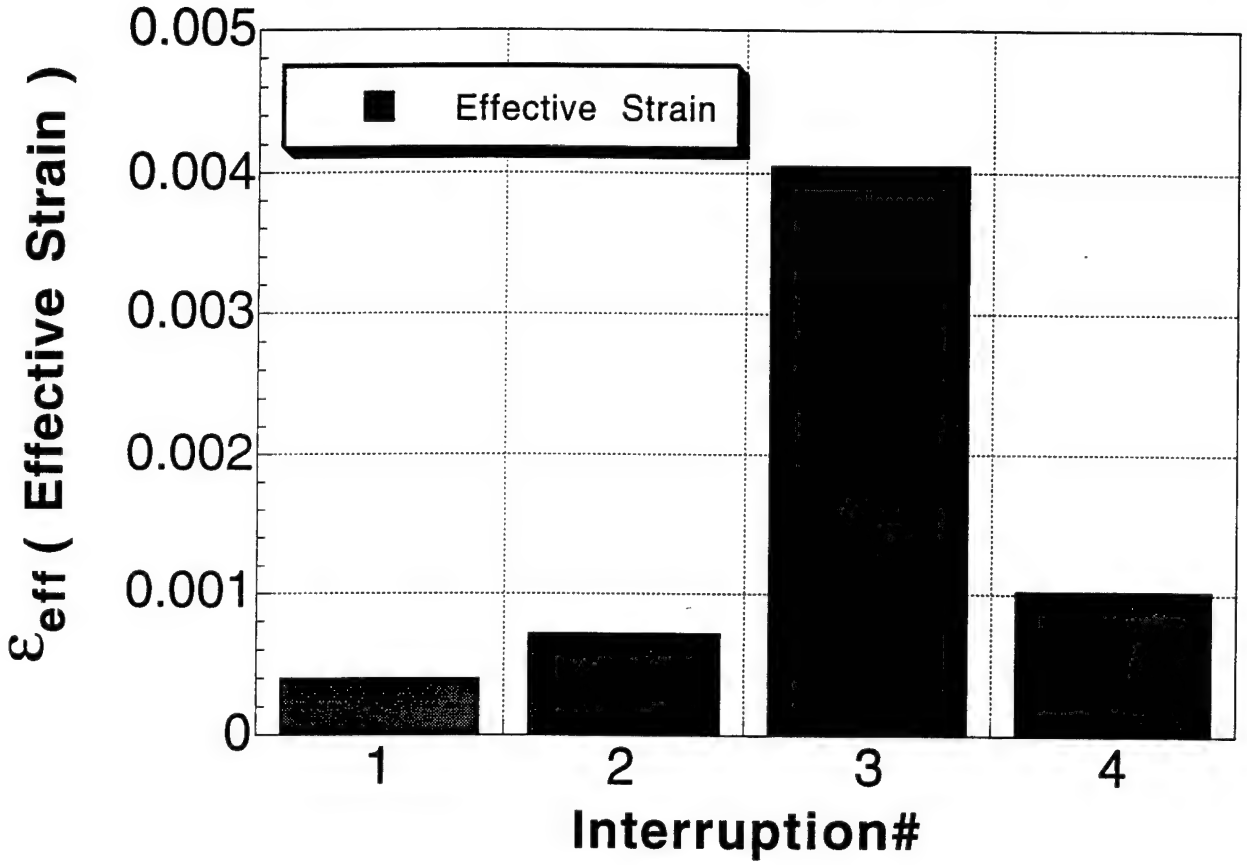

Figure 12) Effective strain gauge measurements of the 3mm copper laminate (s=5.74mm). Deformation occured mainly during interruption#3 when the crack unconstrained the interface allowing copper to flow.

VI. Conclusions

It can be seen in the analysis above that the interface toughness under compression of these offset shear composite specimens offers a wealth of information. The final values for the surface free energy may be questionable, $G_{prop}=85J/_{m^2}$ for the 1mm thick copper and $G_{prop}=312J/_{m^2}$ for the 3mm thick copper laminate. Further study may result in refinement of the analysis used to find the free energy values. It is quite clear that constraint and plasticity within the metal layer plays a role upon the overall interfacial toughness of the specimen since slip within the metal phase can weaken the interface significantly, as $\tau_{max}=36.6$ MPa for the 3mm thick copper layer, as $\tau_{max}=33.2$MPa for the 1mm copper layer laminates indicate, and $\tau_{max}=31.9$MPa and 112MPa for the 25μm thick copper layer laminates with and without a precrack.

The shear constraint factors may be useable as some type of criteria for predicting deformation and failure mechanisms. For the three copper lamiantes characterized in this study, three different modes of deformation were observed at three different constraints. As this phenomena is studied further, it is certainly possible that predictions of failure mechanisms could be quantified.

In analyzing the deformation characteristics of all the laminates along side their corresponding constraint data, it appears that there are two mechanisms, a stress based and a strain based mechanism, working to determine whether or not a crack will initiate along the interface as well as the stress level at which this will occur. At high constraint, as in the case of the 25μm copper laminate, the maximum shear stresses were quite high at 112MPa displaying no slip bands. This behavior contrasts that of the 1mm and 3mm copper laminates which have low constraint and low maximum shear stresses of 33.2 and 33.6MPa with profuse slip band formation. The difference in the mechanism of crack formation in the three laminates is that the amount of strain possible decreases with increasing constraint (or decreasing copper layer thickness) and the corresponding stress

increases with increasing constraint. It gets increasingly difficult for deformation to occur as the constraint gets higher preventing the necessary defect formation at the interface for the crack to nucleate, as in the 25μm copper laminate case. Even in the event of a crack starting out on the interface, the high constraint of the 25μm copper laminate prevented crack propagation along the interface since deformation still could not form ahead of the crack. It is becoming increasingly clear that in order to initiate a crack at the interface there has to be low enough constraint to allow deformation to occur, as in the case of the 1mm and 3mm copper laminates. Thus there has to be minimum levels of strain (to allow slip) and stress (to yield the copper), inorder to nucleate a crack at the interface.

References

[1] Cannon, R. M., Dagleish, B. J., and Dauskardt, R. H., " Crack Path and Fracture Energies in Ceramic-Metal Sandwich Geometries ", prepress Journal of the American Ceramic Society, 1992 pp 16

[2] Charalambides, P. G., Lund, J., and Evans, A. G., " A Test Specimen for Determining the Fracture Resistance of Bimaterial Interfaces ", Journal of Applied Mechanics March 1989 **56** pp 77

[3] Evans, A.G. and Dagleish, B.J.," The Fracture Resistance of Metal-Ceramic Interfaces ", Materials Science and Engineering A **162** 1993 pp 2

[4] Mukai, K. and Ghosh, A.K., " Fundamental Studies on the Mechanical Behavior and Fracture of Metal-Ceramic Interfaces ", AASERT Program report, December 1994

[5] Moya, F., Moya, E. G., and Juvé, D., " SIMS Study of Copper Diffusion into Bulk Alumina ", Scripta Metallurgica et Materialia 1993 **28** pp 347

[6] Beraud, C., Courbiere, M., and Esnouf, C., " Study of Copper-Alumina Bonding ", Journal of Materials Science 1989 **24** pp 4545-4554

[7] Yoshino, Y. and Sibata, T.," Structure and Bond Strength of a Copper-Alumina Interface ", Journal of the American Ceramic Society **75** (10) 1992 pp 2756-2760

[8] Trumble, K.," Thermodynamic Analysis of Aluminate Formation at Cu/Al_2O_3 Interfaces", Acta Metallurgica et Materialia 1992 **40** Suppl. pp s105-110

[9] Bannister, M. and Ashby, M.F., " Ther Deformation anf Fracture of Constrained Metal Sheets ", Acta Metallurgica et Materialia 1991 **39** (11) pp 2575-2582

[10] Hsueh, C.H. and Evans, A.G., " Residual Stresses in Metal/Ceramic Bonded Strips ", Journal of the American Ceramic Society, **68** (5) 1985 pp 241-248

[11] Boyer, H.E. adn Gall, T.L, " Metals Handbook ", American Society for Metals, OH @1985 pp 7•2

[12] Dieter, G. E., " Mechanical Metallurgy ", McGraw-Hill Book Company, London @1988 pp187

[13] Broek, D., " Elementary Engineering Fracture Mechanics ", Martinus Nijhoff Publishers, Dordrecht @ 1986 pp123-140

[14] Barret, C.R., Nix, W.D., and Tetelman, A.S.," The Principles of Engineering Materials ", Prentice-Hall, Inc. NJ @1973 pp247-248

[15] Chin, G.Y., Hosford, W.F., and Mendorff, D.R., Proc. roy. Soc., **A309** 1969 pp 433-56

[16] Ashby, M.F., Blunt, F.J., and Bannister, M.," Flow Characteristics of Highly Constrained Metal Wires ", Acta Metallurgica et Materialia 1989 **37**(11) pp 1847-1857

[17] Underwood, E.E., " Quantitative Metallography ", Metallographic Techniques, 1970 pp 123-134

[18] Ashby, M.F., Phil. Mag., ser.8 **21** 1970 pp 399-424

[19] Hall, E.O., Proc. Phys. Soc. London, 1951 **643** pp 747

[20] Petch, N.J., Iron Steel Inst. London, 1953 **173** pp 25

[21] Wasilewski, R.J., " Deformation Twinning as a Mode of Energy Accomodation ", Metallurgical Transactions, **1** 1970 pp 1333-1335